AMADEUS: Next Generation Materials and Solid State Devices for Ultra High Temperature Energy Storage and Conversion

Alejandro Datas[1, a)], Ana Belén. Cristobal[1], Carlos del Cañizo[1], Elisa Antolín[1], Michel Beaughon[1], Nikolaos Nikolopoulos[2], Aristeidis Nikolopoulos[2], Myrto Zeneli[2], Natalia Sobczak[3], Wojciech Polkowski[3], Merete Tangstad[4], Jafar Safarian[4], Daniele M. Trucchi[5], Alessandro Bellucci[5], Marco Girolami[5], Roman Marx[6], Dominik Bestenlehner[6], Stephan Lang[6], Aniello Vitulano[7], Gianfranco Sabbatella[7], and Antonio Martí[1]

[1]*Solar Energy Institute, Technical University of Madrid, Avda. Complutense 30, 28040 Madrid, Spain.*
[2]*Centre for Research and Technology Hellas, Chemical Process and Energy Resources Institute, Egialias 52, GR-15125 Marousi, Athens, Greece.*
[3]*Foundry Research Institute, Centre for High-Temperature Studies, Zakopiańska 73 Str. 30-418 Cracow, Poland*
[4]*Norwegian University of Science and Technology, Department of Materials Science and Engineering, Alfred Getz vei 2, Trondheim, Norway*
[5] *Istituto di Struttura della Materia (ISM-CNR), Research Area Roma 1, Via Salaria km 29.300, 00015 - Monterotondo Scalo, Rome, Italy*
[6]*University of Stuttgart, Institute of Thermodynamics and Thermal Engineering, Pfaffenwaldring 6, 70569 Stuttgart, Germany*
[7]*Ionvac Process SRL. Viale Anchise, 00040 Colli di Enea, Rome, Italy*

[a)]Corresponding author: a.datas@ies.upm.es

Abstract. Starting in January 2017, AMADEUS (www.amadeus-project.eu) is the first project funded by the European Commission to research on a new generation of materials and solid state devices for ultra-high temperature energy storage and conversion. By exploring storage temperatures well beyond 1000 ºC the project aims at breaking the mark of ~ 600ºC rarely exceeded by current state of the art thermal energy storage (TES) systems. AMADEUS Project, through a collaborative research between seven European partners, aims to develop a novel concept of latent heat thermal energy storage (LHTES) systems with unprecedented high energy density. One of the main objectives of the project is to create new PCMs (phase change materials) with latent heat in the range of 1000-2000 kWh/m^3, an order of magnitude greater than that of typical salt-based PCMs used in concentrated solar power (CSP), along with developing advanced thermal insulation, PCM casing designs, and novel solid-state heat to power conversion technologies able to operate at temperatures in the range of 1000-2000 ºC. In particular, the project will investigate Silicon-Boron alloys as PCMs and hybrid thermionic-photovoltaic (TIPV) devices for heat-to-power conversion. This paper describes the project R&D activities and the main results that have been attained during the first 6 months of work. This includes the first wettability and solubility analysis of liquid Si-B alloys, the numerical simulation of silicon phase-change and heat loss analysis through thermal insulation cover, as well as the first steps for the realization of the two main AMADEUS proof-of-concept experiments: the TIPV converter, and the full LHTES device.

SolarPACES 2017
AIP Conf. Proc. 2033, 170004-1–170004-10; https://doi.org/10.1063/1.5067168
Published by AIP Publishing. 978-0-7354-1757-1/$30.00

INTRODUCTION

Solar thermal energy storage based on very high melting point PCMs, such as pure silicon and boron (melting points of 1414 ºC and 2076 ºC), plus solid state energy conversion has been proposed theoretically in the past [1]–[5], the main motivation being the extremely high latent heat and thermal conductivity of these PCMs if compared with salt-based materials. Figure 1 (a) shows the latent heat of fusion of different materials as a function of the melting temperature, illustrating the particular potential of silicon (1230 kWh/m^3) and boron (2680 kWh/m^3), having latent heats an order of magnitude greater than that of typical salts used in CSP such as $NaNO_3$ (110 kWh/m^3) and KNO_3 (156 kWh/m^3). Actually, silicon and boron PCMs provide higher storage energy densities than most forms of energy storage, including electrochemical batteries and pressurized hydrogen (Figure 1a).

The obvious technological challenge is the very high operation temperature, especially concerning the heat-to-power conversion system. Maximum operation temperatures of conventional dynamic closed-cycle engines such as closed-Brayton, Stirling and Rankine, are typically well below 1000 ºC [6]. This is mostly because of the very serious concerns with the working fluid stability and structural mechanical strength of the engine steel parts at high temperatures. On the contrary, solid state converters, such as thermionics (TI) [7] and thermophotovoltaics (TPV) [8], [9] are perfectly suited for such high temperatures, mainly because they are based on the direct emission of electrons and photons through a vacuum space, eliminating the need of working fluid and moving parts. AMADEUS project represents the first attempt to develop latent heat thermal energy storage (LHTES) based on ultra-high temperature PCMs and solid state heat-to-power converters.

AMADEUS PROJECT OBJECTIVES

Under the coordination of IES-UPM, AMADEUS, counts with the participation of seven European partners with experience in the fields of high temperature materials (NTNU and FRI), fluid-dynamics and finite elements analysis (CERTH), thermal insulation (USTUTT), and solid state heat-to-power conversion based on thermionics (CNR and Ionvac) and photovoltaics (IES-UPM). The project is divided in two main blocks (Figure 1b): high temperature heat storage, and high temperature energy conversion. Both blocks will thoroughly investigate each part of a system that will be eventually built and tested at the end of the project. To that end, the technologies that are investigated are:

- Novel PCMs based on the silicon-boron system with ultra-high melting temperature and latent heat.
- Novel refractory lining composites based on carbides, nitrides and oxides for the PCM container walls.
- Advanced thermally insulated PCM casing enabling small heat losses.
- Proof of concept of a novel hybrid thermionic-photovoltaic (TIPV) device [10].
- Proof of concept of the final complete LHTES device comprising the elements described above.

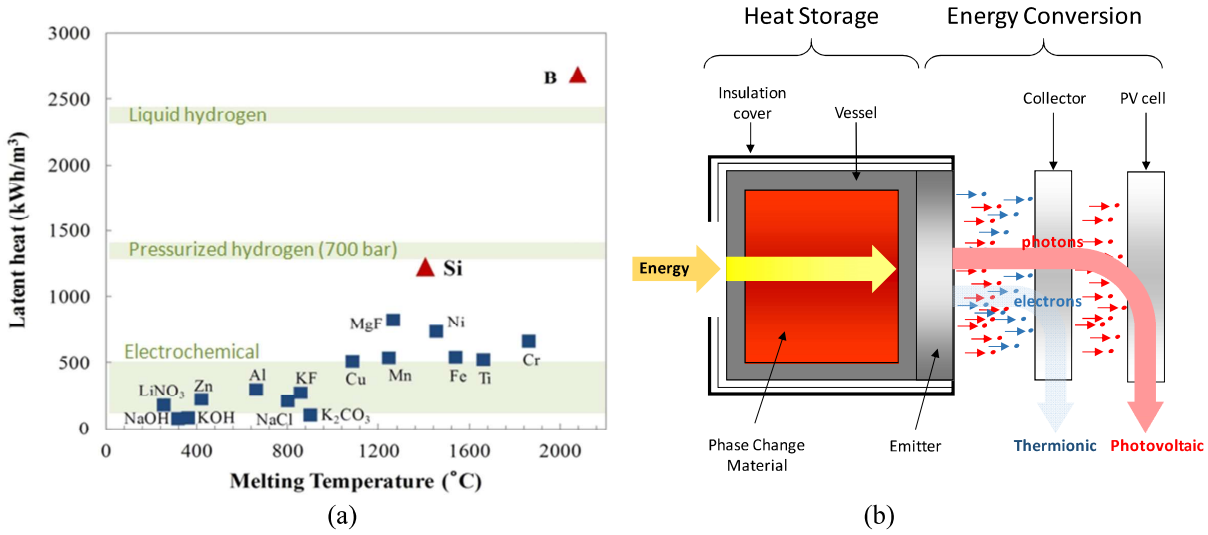

(a) (b)

FIGURE 1. (a) Latent heat of fusion of different materials as a function of melting temperature compared with the energy density of other storage technologies, (b) sketch of the final AMADEUS storage system.

AMADEUS project has a budget of 3.3 M€ for the next 3 years and the final aim is to demonstrate the proof-of-concept of this new energy storage and conversion concept.

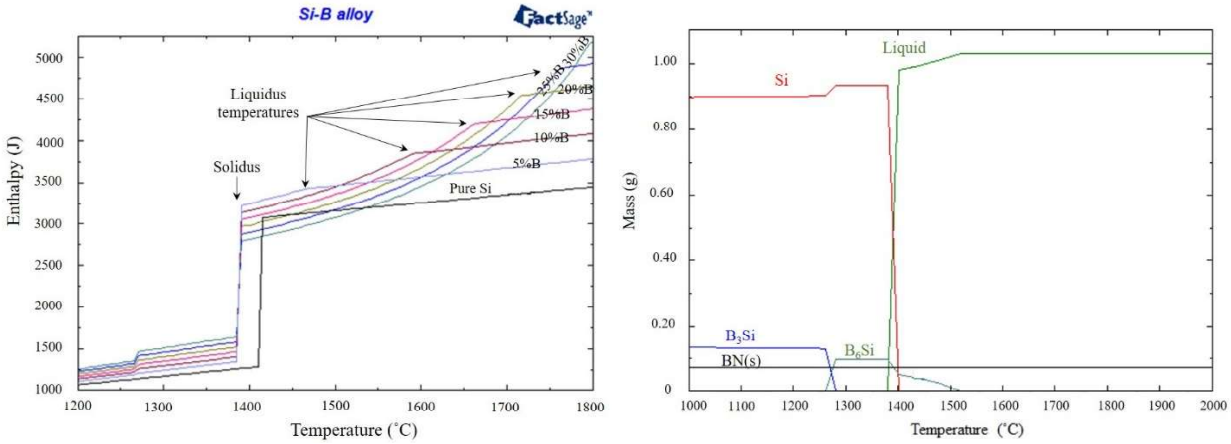

FIGURE 2. (a) The enthalpy changes for Si and selected Si-B alloys at elevated temperatures. (b) The calculated stable phases for the interaction of one gram Si-10%B alloy with 0.1 g Si_3N_4 crucible at different temperatures.

ULTRA-HIGH TEMPERATURE HEAT STORAGE

This section describes the Project activities on the heat storage block (see Figure 1b). This includes $SixB1_{-x}$ PCM, PCM-container interaction, heat transfer during the melting/solidification of the PCM, and thermal insulation.

Silicon-Boron based PCMs

The selection of proper Si-B alloys and the alloys container material at elevate temperatures is studied through experimental and theoretical thermodynamic work.

The latent heat of fusion for pure Si and B elements are significantly larger than the other common metals as illustrated in Figure 1a. Therefore, the application of Si-B binary alloys as the ultra-high temperature PCMs is a smart choice as it is possible to provide molten Si-B alloys in temperatures significantly lower than the melting point of B (2076˚). Different types of borides can be found in literature between Si and B, however in a wide compositional range up to 85 at% B, two main borides exist, SiB_{4-x}, and SiB_6. The x-value in SiB_{4-x} is smaller than unity and it is close to 1 at 1270˚C, the highest temperature that this phase is stable. In the temperature range of 1270-1385˚C the SiB_6 is stable, while a solid solution of B in Si co-exists with it for alloys with up to 85 at%B. The solubility of B in this silicon phase is increased with increasing temperature up to around 3 at% as the maximum solubility at 1385˚C, which is the eutectic isotherm on the silicon rich part of the Si-B system [11]. Considering the main objective of the AMADEUS project, the silicon-rich part of the Si-B system is of interest, as there is a better heat storage possibility and also fewer problems regarding the alloys interaction with the container at high temperatures.

In order to study the proper Si-B alloy candidates, the enthalpy changes for Si-B alloy systems were studied using the FactSage thermodynamic software and the results are shown in Figure 2a. As we see, the overall enthalpy changes in a given temperature range depends on the composition of the alloy and there is higher enthalpy changes for Si-B alloys compared to pure silicon. It is worth mentioning that the liquid solutions of Si-B alloys show positive deviation from ideal solution and there is positive enthalpy of mixing for this system. Figure 2a shows that for all selected Si-B alloys with more than 5 wt%B, the solidus is lower than the silicon melting point, which is actually the eutectic temperature in the system. Moreover, the enthalpy change at this temperature depends on the B concentration in the alloy and for the considered lowest B concentration of 5 wt%B, larger enthalpy change is observed at the solidus temperature. It may be concluded that the alloys closer to the eutectic point on Si-B system are better candidates as they show larger enthalpy of fusion at solidus, while they show almost the same rate of enthalpy changes with temperature as higher B concentrations above the liquidus temperature (Figure 2a). It may be

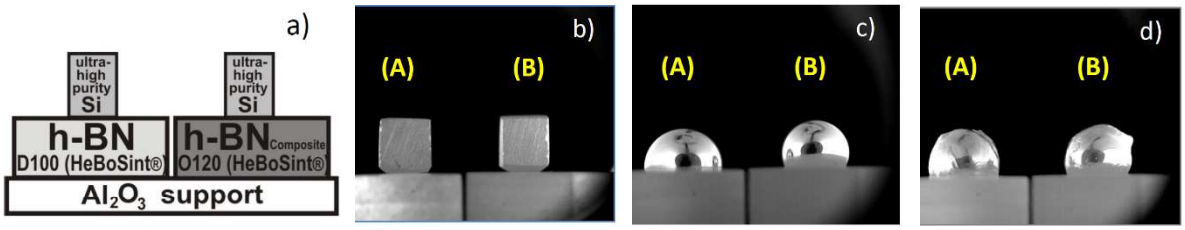

FIGURE 3. Exemplary images in-situ recorded during wettability tests by new sessile drop method coupled with contact heating procedure: a) a schematic drawing of the Si/h-BN couples; b) two couples at 1200°C (below melting point of Si); c) a drops formation at temperatures higher than melting point of Si (1750°C); d) solidified couples after cooling down to 1300°C. (couple A: Si/h-BN, couple B: Si/h-BN+SiC+ZrO2 composite). For both couples non-wetting behavior was maintained at temperature up to 1750 °C, but higher contact angle values were recorded for the h-BN based composite.

beneficial to use Si-B alloys with compositions close to the eutectic point in the Si-B system where SiB_6 phase and Si solid solution are formed upon cooling and solidification.

PCM-Container Interaction

The considered main Si and B elements are active elements and they are susceptible to oxidation, nitration and carburization in contact with O, N, and C containing solid materials and even gases. On the other hand, oxides, nitrides, and carbides are the most important high temperature refractory materials and the candidate materials to hold Si-B alloys. Therefore, the behavior of different refractories in contact with liquid Si-B alloys and their behavior upon cooling, solidification, and re-melting are crucially important.

For instance, a key parameter may be the solubility of the elements from refractory materials into the molten Si-B alloys and their effects on both the alloy composition and formation of new phases in the system with temperature change. Figure 2b shows a typical equilibrium situation calculated by FactSage for the melting of a Si-10wt%B alloy in a silicon nitride crucible. The graph shows that boron nitride is formed and is a stable solid phase in contact with a molten Si-B alloy at high temperatures. The graph shows also the temperature ranges that different types of silicon borides are stable. In AMADEUS project, the thermodynamics issues related to the interaction between Si-B alloys and candidate materials are investigated through high temperature experimental studies at NTNU and employing thermodynamics calculations. As the multi-component alloy systems containing Si and B elements have not been significantly studied, the project will expand the fundamental knowledge in this area.

Another crucial parameter determining the interaction between refractories and liquid Si-B alloys is their wettability. In this field, FRI is performing a pioneering experimental research on silicon based materials (silicon and Si-B alloys) in terms of their wettability and reactivity with refractories at ultra-high temperatures up to 1750 °C. It is a general rule that in the liquid metal/ceramic systems a good wetting is usually assisted by a high reactivity. These high temperature phenomena result in change of chemistry and structure of contacting materials and finally contribute to a gradual degradation of both metal and ceramic materials (i.e. comes from either a dissolution of crucible and/or formation of reaction products at the interface). Thus, regarding a successful achievement of long lifetimes of the final PCM container, it is a matter of crucial importance to select refractory materials that are non-wetted (i.e. the contact angle $\theta>90°$) by molten silicon and its alloys. Based on conducted literature survey, it has been found that most of commonly used in practice oxides, carbides or nitrides are well wetted by pure Si. In fact, the only one ceramic showing non-wetting behavior in contact with molten Si at temperature around its melting point is hexagonal boron nitride (h-BN) [12]–[14]. It has to be noted that there is a complete lack of reported information about the high temperature interaction of refractories with both pure Si and Si-B alloys at temperatures higher than 1500 °C. Moreover, the results of conducted preliminary high temperature measurements of thermophysical properties of selected PCM candidates have clearly pointed toward a strong chemical interaction of both Si and Si-B alloy with crucible materials such Al_2O_3 and graphite, widely used in container assisted methods (e.g. calorimetry, dilatometry). Therefore, it has been concluded that ultra-high temperature wettability tests are very important in order to select new refractories not only for the construction of PCM container in LHTES system, but also regarding a successful implementation of any container-assisted laboratory technique for high temperature measurements of thermophysical properties of Si-based alloys.

The wettability tests have been performed by using a unique experimental complex for investigations of high temperature capillarity phenomena located in FRI (more details on the apparatus are shown elsewhere [15], [16]).

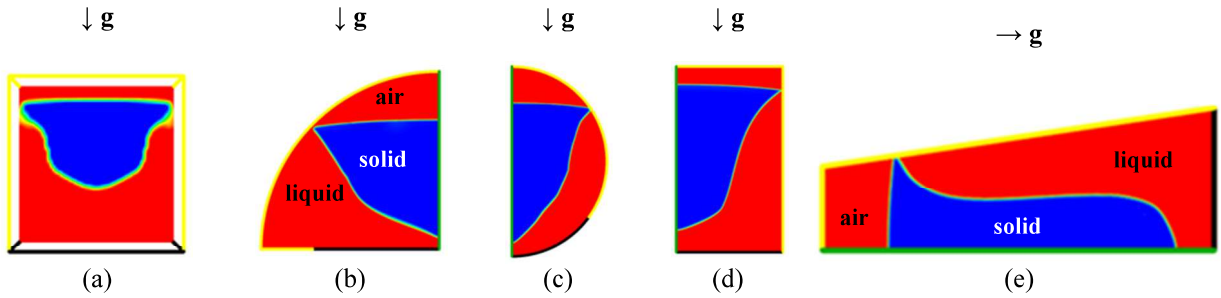

FIGURE 4. Results for the simulation of the process of melting pure silicon using ANSYS Fluent platform (v17.1). Comparison of the melt fractions contours (blue means "solid", red means "fluid") at t=20 min for the five different designs: a) cube, b) half-sphere, c) sphere, d) cylinder, e) truncated-cone. In the contours figures with green is indicated the axis, with yellow the walls and black the emitter surface. In these transient simulations, the Courant number is equal to 0.2, Amush=105 (ANSYS Fluent default). IN these simulations, the assumed silicon properties are: $T_{solidus}$ = 1686 K, $T_{liquidus}$ =1688 K, L= 1800 kJ/kg, ρ=2330 kg/m3 (solid), ρ=2570 kg/m3 (liquid), k=25 W/m-K (solid), k=50 W/m-K (liquid), Cp = 1040 J/kg-K (solid and liquid). Air is assumed compressible-liquid (Tait equation) with: k=0.0573 W/m-K, Cp = 1189 J/kg-K, μ = 4.96 kg/m-s.

Four different types of h-BN based materials have been used for the wettability examinations: bulk h-BN sinters fabricated by using sintering aids (B_2O_3), bulk h-BN sinters fabricated without using sintering aids, bulk h-BN+SiC+ZrO_2 composite sinters and h-BN spray slurries. The results of experiments (see examples in Figure 3) allow drawing the following preliminary conclusions: (1) All examined h-BN based materials show non-wetting behavior in contact with molten silicon at temperatures up to 1650 °C while non-wetting-to-wetting transition (θ<90°) with pure Si and pure h-BN takes place at higher temperature, (2) The h-BN+SiC+ZrO_2 composite shows the most promising behavior in contact with molten Si at the whole testing temperature range (θ=145-115° at 1450-1750°C, respectively). (3) The h-BN spray deposited on SiC polycrystalline substrate (for Si/SiC, θ~40°) showed non-wetting behavior with molten Si even at T=1750°C. However, a rather poor adhesion of coatings was observed after cooling down the systems to room temperature, what brings serious doubts about their thermal cycling resistance.

The structure and chemistry of solidified couples are now under investigations by means of optical microscopy, scanning electron microscopy, scanning probe microscopy, Raman spectroscopy and computed tomography, in order to elucidate involved phenomena and mechanisms of metal/ceramic interactions at ultra-high temperatures.

Heat Transfer Analysis in the PCM

A CFD model simulating the complex heat transfer mechanisms occurring inside the Silicon-Boron PCM is being formulated so that it can be used as a powerful tool both for its design phase and its further optimization. The model simulating the PCM is based on the ANSYS Fluent platform [17] and integrates the multiphase volume of fluid (VOF) approach, coupled with an adaptive local grid refinement technique, capable of achieving a sharp interphase, and a solidification-melting approach able to model the solid/liquid transition in the under examination LHTES system. The last approach is based on the enthalpy-porosity method [18]. Initially, the model is validated for the melting of paraffin wax inside a spherical casing. Experimental data are retrieved from the open literature concerning various melting fraction values at different time instants [19]. For most of the simulation time the numerical results of the applied CFD model almost coincide with the corresponding numerical predictions of the reference paper and are close enough to the experimental data. However, through a parametric numerical analysis it was found that the mushy zone parameter affects significantly the melting process of the PCM and its effect on the melting rate should be further investigated. This parameter is dependent on the dendrites formed during the solidification process, the material density and viscosity, parameters that reflect in turn the PCM permeability. A grid dependency study is also conducted by using a refinement technique [20], in which numerous in-house user-defined functions (UDFs) have been implemented. Almost identical results are obtained for the three different grid densities tested, however, the local refinement is preferred over the uniform grids, as it increases the CFD model accuracy, especially in the liquid-solid interphase.

The validated CFD model with the local refinement technique (10,000 cells) has been used to simulate the melting process of pure silicon inside a closed casing heated from the walls at a uniform temperature of 2000 K. Solid PCM is patched in 95 % of the whole domain, with the rest of it being filled with air, treated as compressible

fluid in order to take into account the development of realistic pressure fields for the case that an venting valve is not used in the encapsulation vessel. Five casing designs, cube, truncated cone, sphere, half sphere and cylinder, all with the same volume and emitter surface, i.e. 0.03375 m^3 and 0.0225 m^2 respectively, are simulated to test their effect on the PCM melting rate. From Figure 4 we observe that there is a significant effect of the casing shape on the PCM melting process. As expected, the melting process is the slowest in the sphere (~40 minutes) and the fastest in the cube and truncated cone (~ 26-28 min), due to the lower surface to volume ratios in the sphere case. In all cases the solid phase floats in the molten PCM during the melting process, as expected due to the lower solid PCM density than that of molten PCM. The induced stresses during the thermal expansion of the PCM will be analyzed in future simulations using Finite Element Models (FEM) to provide recommendations on the optimal container geometries.

Thermal Insulation

The first step towards the development of a thermal insulation for the ultra-high temperature latent heat thermal energy store (TES) was a research for suitable thermal insulation materials (TIMs). It was found that TIMs, which can stand temperatures up to 2 000 °C, are significantly more expensive than TIMs for lower temperatures. Furthermore there are TIMs, which can stand temperatures up to 1 000 °C, with significantly lower thermal conductivities than TIMs for ultra-high temperatures (> 1 000 °C). Thus, the first insulation concept considered is a multi-layer thermal insulation consisting of commercially available TIMs. In this concept only the inner insulation layer must stand temperatures up to 2 000 °C. As content of the outer insulation layers, TIMs with lower costs and lower thermal conductivities can be used. Thus, the costs, the heat losses and the total insulation thickness can be reduced compared to one-layer insulation concepts. The whole assembly must be enclosed in a gas-tight casing to provide the possibility of creating an atmosphere of inert gases or vacuum.

With this insulation concept and the parameters of the researched TIMs, thermal simulations with the software COMSOL Multiphysics 5.2a were performed. In the simulations the TIMs, the thicknesses of the insulation layers and the gas in the gap between the TES and the TIMs as well as in the pores of the TIMs were varied. The resulting heat loss rates and temperature propagations were evaluated.

The TES and its multi-layer insulation concept, as it was modeled for the simulations, are illustrated in Figure 5. The TES model was built up as a truncated cone with diameters of 150 and 100 mm and a height of 150 mm, and is consisting of the storage material and the container. It is surrounded by a gap that contains air, argon or high vacuum respectively and by two to three cylindrical insulation layers. It is fixed by four cylindrical support stacks, which extend half its thickness into the inner insulation layer. The TES is modeled as a solid body with a constant temperature of 2026.85 °C (2300 K). The ambient temperature is 30 °C.

As a result of the simulations the application of vacuum in the thermal insulation was found to be very promising in order to reduce both insulation thickness and heat losses, and consequently costs. A two-layer insulation of graphite fiber mat and fumed silica board with a total thickness of 540 mm in argon atmosphere resulted in a total heat loss rate of 755 W. The same two-layer insulation with even smaller total thickness of 500 mm in vacuum resulted in a significantly lower total heat loss rate of 370 W.

Further information on the researched TIMs, the simulation model, the simulation results, and the costs of the insulation concepts can be found in [21].

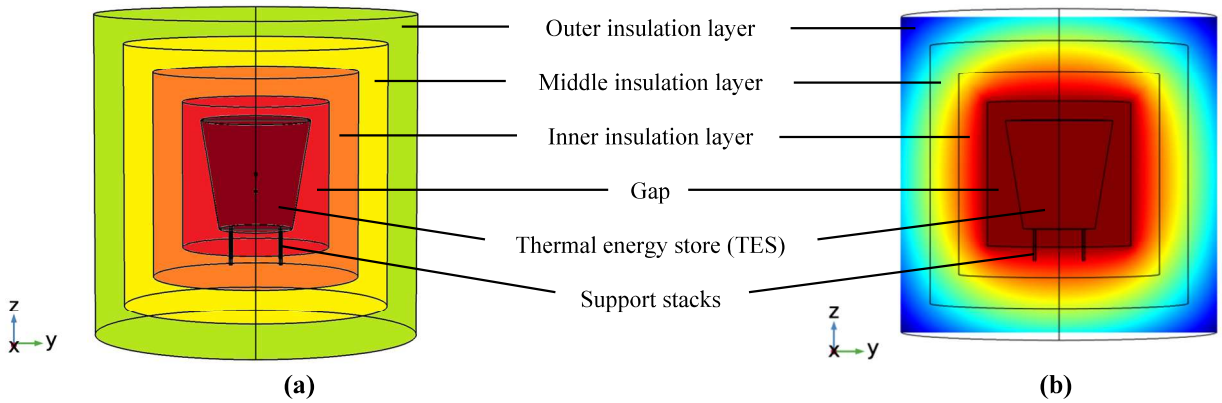

FIGURE 5. Thermal insulation concept with three insulation layers. a) 3D sketch; b) thermographic image of a zy-plane cut through the center of the thermal energy store.

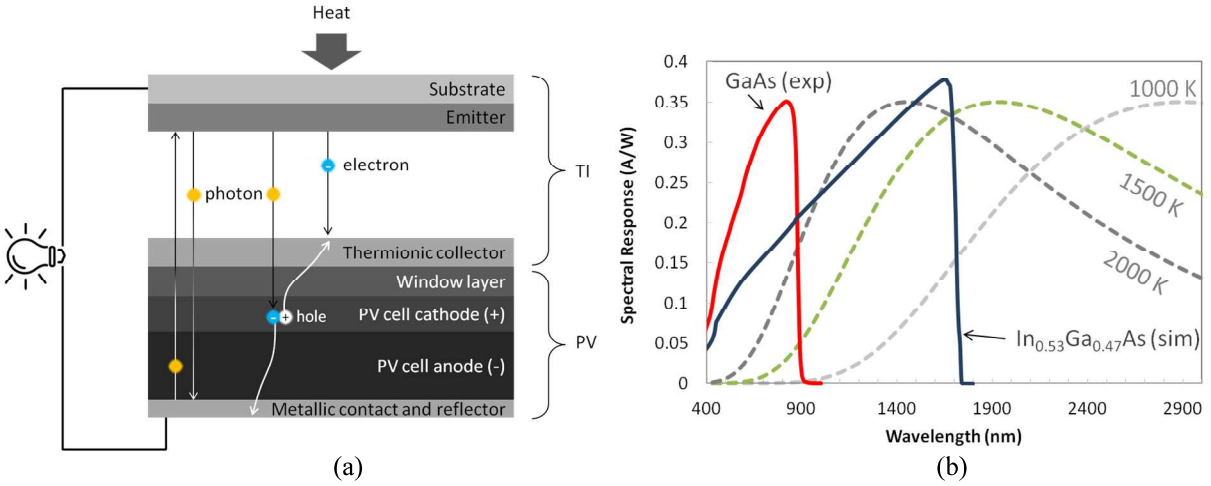

FIGURE 6. (a) The thermionic-photovoltaic (TIPV) device, (b) PV cell spectral response together with black-body spectrum (represented PV cells do not have anti-reflective coatings).

ULTRA-HIGH TEMPERATURE HEAT-TO-POWER CONVERSION

This section describes the Project activities concerning the energy conversion block (see Figure 1b) which basically consist of realizing the proof of concept of a novel hybrid thermionic-photovoltaic (TIPV) device. Both thermionic (TI) and infrared photovoltaic (PV) or thermophotovoltaic (TPV) have been demonstrated to be feasible for many high temperature energy conversion applications. In particular, the research teams participating in this project have already successfully demonstrated these two separate technologies for concentrated solar applications: solar-thermionics at CNR [22] and solar-thermophotovoltaics at IES-UPM [23].

AMADEUS project will investigate TIPV devices, which have been recently formulated theoretically by one of the authors of this article [10]. TIPV devices consist of a tandem arrangement between a thermionic and a photovoltaic cell (Figure 6a). The TIPV device comprises two main elements: the TIPV cathode (or emitter) and the TIPV anode (comprising the thermionic collector and the PV cell). The TIPV emitter is designed to have low work function and high optical emissivity; thus when heated, it radiates two kinds of energy carriers: electrons and photons. Electrons are absorbed by the thermionic collector (which has a lower work function than the emitter) and photons pass through the transparent collector to be absorbed in the PV cell, generating an electron-hole pair. The electrons absorbed in the thermionic collector recombine with holes coming from the PV cell cathode; thus closing the circuit and series connecting the thermionic and photovoltaic sub-devices. The photons that are not absorbed in the PV cell (e.g. those with too long wavelength) may be reflected in a back-side mirror and turned back to the emitter, not representing a loss of energy. Finally, the emitter and the PV cell anode are externally connected to deliver an external electrical power. Due to the action of two heat carriers, this combination provides a notable increment of the power density with respect to the independent thermionic and photovoltaic devices.

TIPV Cathode

The TIPV cathode is the hot side of the converter and consists of a substrate – which represents the interface with the thermal energy storage tank, expected to work at an operating temperature as high as 2000 °C – matched with a specific thin (10 - 100 nm) emitting layer, able to efficiently emit electrons, to be collected by the thermionic collector, and a photon flux, to be absorbed by the underlying thermophotovoltaic (TPV) cell. Since the recent years, the DiaTHEMA (Diamond, Thermal & Harsh Environment Materials & Applications) laboratory at CNR has been preparing black diamond based high temperature (<800 °C) solar cells based on photon-enhanced thermionic emission [24], [25]. However, the specifications of the AMADEUS project are even more ambitious in terms of operating temperature. In order to choose the appropriate substrate and emitter materials, a number of requirements must be taken into account. The substrate should be characterized by: 1) a melting point > 2000 °C; 2) a large thermal conductivity for a suitable heat transfer towards the emitting layer; 3) thermal stability at operating

temperatures; 4) a very low electric resistivity (10^{-4} - 10^{-5} Ω cm) to avoid bottlenecks for electron refilling from the external circuit, namely to ensure a low cathode series resistance; 5) a coefficient of thermal expansion comparable to that of the emitting layer, in order to achieve a good adhesion and ensure thermal stress relief; 6) an absorption coefficient matched with the storage tank if the energy is exchanged by thermal irradiance.

The characteristics of the emitting layer are related to the enhanced capability to emit electrons and to its optical properties, which should be able to satisfy the specific requirements of the PV cell in terms of radiation absorption. The emitter should have: 1) a high melting point to sustain the operating temperature; 2) a work function ϕ_E as low as possible (<2.7 eV), but at the same time matched with the collector one ϕ_C (it must be indeed $\phi_E > \phi_C$ to ensure a proper power generation); 3) a spectrally selective emissivity matched with the PV cell, i.e. high (low) emissivity for wavelengths smaller (larger) than the wavelength corresponding to the bandgap of the PV cell active material; 4) a coefficient of thermal expansion comparable to that of the substrate, in order to achieve a good adhesion and ensure thermal stress relief. Refractory metals have been individuated as suitable candidates for the thermionic emitter substrate, whereas several boride, carbide, nitride films are under investigation and development by physical and chemical vapor deposition techniques to obtain low-work-function emitters.

TIPV Anode

The TIPV anode is the cold side of the TIPV converter and comprises the PV cell and the thermionic collector layer (see Figure 6). Infrared sensitive semiconductors, with bandgap energies below ~ 0.75 eV must be used to fabricate the PV cell, in order to capture the infrared spectrum radiated by the emitter. In particular, the cathode (anode) of the PV cell will be made of p-doped (n-doped) $In_{0.53}Ga_{0.47}As$ semiconductor (bandgap of 0.74 eV). A partially transparent p-doped window layer made of InAlAs (bandgap of ~ 1.45 eV) will be grown on top of the PV cell cathode to fabricate a selective contact for holes and provide a good surface passivation. With the same purpose, an n-doped InAlAs back surface field (BSF) layer will be incorporated below the PV anode. The full semiconductor structure will be grown by Molecular Beam Epitaxy (MBE) on InP substrates by IES-UPM. This structure will be eventually transferred to CNR for thermionic collector coating. The thermionic collector has to guarantee a very low work function, thermal stability at the anodic operating temperatures (desired to be <100 °C), and transparent to the radiation emitted by the emitter and exploited by the underlying TPV cell. To satisfy these requirements, very thin (<2 nm) barium composite coatings are under development at CNR by physical deposition methods.

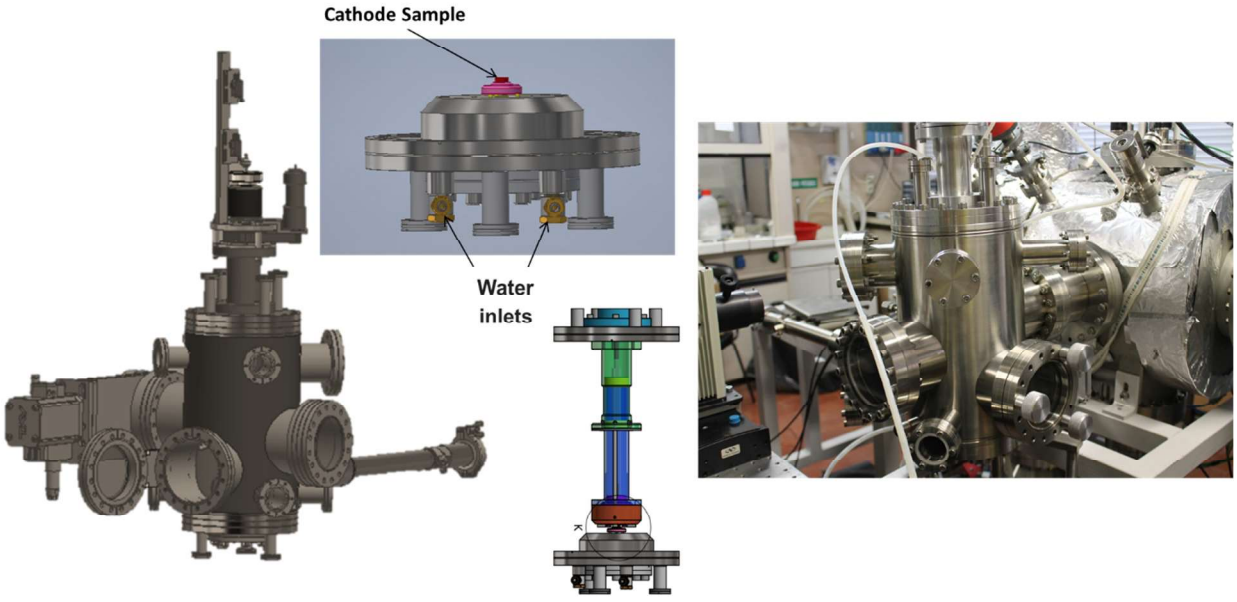

FIGURE 7. a) CAD design of the experimental setup: on the right, a description of the cathode holder (above) and of the moving parts for approaching the anode to the cathode (below). b) Installation of the AMADEUS experimental setup on the UHV analysis chamber.

Preliminary experiments have been started on GaAs semiconductor. Figure 6b shows the normalized black-body emission spectrum along with the spectral response of both GaAs (experimental) and $In_{0.53}Ga_{0.47}As$ (simulated using PC1D) PV cells, showing the better spectral match of the $In_{0.53}Ga_{0.47}As$ device. However, GaAs structures will be used first due to the readiness level of the technology. Using these structures, PV power densities as high as ~ 0.2 W/cm^2 (GaAs) and ~ 3 W/cm^2 (InGaAs) would be expected for emitter temperatures of ~1400ºC. This is 10 and 150 times greater than conventional solar cells (~ 0.02 W/cm^2). Notice that this result does not consider anti-reflective coatings on the cell and assume black body emission (emissivity = 1); thus, corrections to these predictions must be done taking into the actual optical properties of the final device surfaces.

FINAL PROOF-OF-CONCEPT EXPERIMENTS

The final goal of AMADEUS project is to realize two proofs of concepts: (1) the TIPV device, and (2) the full LHTES device. The later activity will start near the end of the project, when all the other elements have been properly defined. However, the activities concerning the TIPV proof of concept have already started. Therefore, in this section we introduce the experimental setup that has been developed to characterize materials and to evaluate performances of TIPV devices.

In order to reach the AMADEUS ultra-high operating temperatures (T_{op} = 2,000 °C), the vacuum system has been accurately designed by CNR and IONVAC for integrating materials thermally stable at temperatures up to 2000ºC and carefully managing the thermal flows (Figure 7). The main features of the setup are: 1) the control of the distance between the electrodes with a sub-micrometric resolution o 0.5 μm, 2) the cooling system driven also by liquid nitrogen for maintaining the PV cell to room temperature, and 3) the possibility to perform in-situ depositions by thermal evaporation for engineering the anode surface (it means to lower the anode work function). Figure 7 shows the installation of the experimental setup on an ultra-high-vacuum (UHV) system (pressure below 10^{-8} mbar). As thermal source, the Lumics LU0808C250-NF0BN high-power laser diode (maximum radiation power of 250 W and operating at a wavelength of 808 nm) is used to provide the suitable radiation power for making the receiver of the TIPV module (i.e. the cathode of the thermionic stage) able to reach the operation temperature.

SUMMARY AND CONCLUSIONS

Starting in January 2017, AMADEUS project is the first European initiative to develop a new generation of materials and solid state devices for ultra-high temperature (>1000ºC) latent heat energy storage and conversion. This paper describes the main project activities along with the main achievements during the first six months of development. The project is divided in two main blocks: heat storage, and energy conversion. Concerning heat storage block, silicon-boron alloys are being investigated to eventually lead to new PCMs with storage energy densities greater than 1000 kWh/m^3. The precise Si_xB_{1-x} composition, along with its interaction with containment vessel, advance thermal insulation materials and heat transfer analysis during the melting/solidification process, are some of the main activities that are being investigated within this project. Concerning the energy conversion block, a new concept for a solid-state heat-to-power conversion, named hybrid thermionic photovoltaics (TIPV), is under investigation. This new device is able to operate at very high temperatures, well above 1000ºC, and provides very high output power densities near or beyond 10 W/cm^2. Thus, both heat storage and energy conversion blocks combined will eventually lead to a new generation of extremely compact LHTES devices. The proofs of concept of the TIPV, as well as that of the full LHTES system, are currently under development within the project.

ACKNOWLEDGEMENTS

The project AMADEUS has received funds from the European Union's Horizon2020 research and innovation program, FET-OPEN action, under grant agreement 737054. The sole responsibility for the content of this publication lies with the authors. It does not necessarily reflect the opinion of the European Union. Neither the REA nor the European Commission are responsible for any use that may be made of the information contained therein.

REFERENCES

[1] D. L. Chubb, B. S. Good, and R. A. Lowe, "Solar thermophotovoltaic (STPV) system with thermal energy storage," 1995, pp. 181–198.

[2] A. Datas, D. L. Chubb, and A. Veeraragavan, "Steady state analysis of a storage integrated solar thermophotovoltaic (SISTPV) system," *Sol. Energy*, vol. 96, pp. 33–45, 2013.

[3] M. R. Reid, D. B. Scharfe, and R. N. Webb, "Computational evaluation of a latent heat energy storage system," *Sol. Energy*, vol. 95, pp. 99–105, Sep. 2013.

[4] A. Veeraragavan, L. Montgomery, and A. Datas, "Night time performance of a storage integrated solar thermophotovoltaic (SISTPV) system," *Sol. Energy*, vol. 108, no. 0, pp. 377–389, Oct. 2014.

[5] A. Datas, A. Ramos, A. Martí, C. del Cañizo, and A. Luque, "Ultra high temperature latent heat energy storage and thermophotovoltaic energy conversion," *Energy*, vol. 107, pp. 542–549, Jul. 2016.

[6] A. Datas and A. Martí, "Thermophotovoltaic energy in space applications: Review and future potential," *Sol. Energy Mater. Sol. Cells*, vol. 161, pp. 285–296, Mar. 2017.

[7] G. N. Hatsopoulos and E. P. Gyftopoulos, *Thermionic Energy Conversion*, 2 vols. Cambridge, Massachusetts: The MIT Press, 1979.

[8] T. Bauer, *Thermophotovoltaics: Basic Principles and Critiical Aspects of System Design*. Springer, 2011.

[9] D. L. Chubb, *Fundamentals of thermophotovoltaic energy conversion*. Elsevier, 2007.

[10] A. Datas, "Hybrid thermionic-photovoltaic converter," *Appl Phys Lett*, vol. 108, no. 14, p. 143503, Apr. 2016.

[11] A. I. Zaitsev and A. A. Kodentsov, "Thermodynamic properties and phase equilibria in the Si-B system," *J. Phase Equilibria*, vol. 22, no. 2, p. 126, Apr. 2001.

[12] Z. Yuan, W. L. Huang, and K. Mukai, "Wettability and reactivity of molten silicon with various substrates," *Appl. Phys. A*, vol. 78, no. 4, pp. 617–622, Mar. 2004.

[13] B. Drevet, R. Voytovych, R. Israel, and N. Eustathopoulos, "Wetting and adhesion of Si on Si3N4 and BN substrates," *J. Eur. Ceram. Soc.*, vol. 29, no. 11, pp. 2363–2367, Aug. 2009.

[14] B. Drevet and N. Eustathopoulos, "Wetting of ceramics by molten silicon and silicon alloys: a review," *J. Mater. Sci.*, vol. 47, no. 24, pp. 8247–8260, Dec. 2012.

[15] N. Sobczak, R. Nowak, W. Radziwill, J. Budzioch, and A. Glenz, "Experimental complex for investigations of high temperature capillarity phenomena," *Mater. Sci. Eng. A*, vol. 495, no. 1, pp. 43–49, Nov. 2008.

[16] N. Sobczak, R. Nowak, J. Budzioch, and A. Glenz, "Experimental laboratory stand for examinations of high temeparture interaction of metals and alloys with refractory materials under isothermal and non-isothermal conditions," 225228.

[17] "ANSYS 17.0 Theory Guide," 2016.

[18] V. R. Voller, M. Cross, and N. C. Markatos, "An enthalpy method for convection/diffusion phase change," *Int. J. Numer. Methods Eng.*, vol. 24, no. 1, pp. 271–284, Jan. 1987.

[19] E. Assis, L. Katsman, G. Ziskind, and R. Letan, "Numerical and experimental study of melting in a spherical shell," *Int. J. Heat Mass Transf.*, vol. 50, no. 9, pp. 1790–1804, May 2007.

[20] I. Malgarinos, N. Nikolopoulos, and M. Gavaises, "Coupling a local adaptive grid refinement technique with an interface sharpening scheme for the simulation of two-phase flow and free-surface flows using VOF methodology," *J. Comput. Phys.*, vol. 300, pp. 732–753, Nov. 2015.

[21] S. Lang, R. Marx, and H. Drück, "Thermal insulations for an ultra-high temperature thermal energy store for concentrated solar power," presented at the SolarPACES 2017, Santiago de Chile, Chile, 2017.

[22] A. Bellucci *et al.*, "Preliminary characterization of ST2G: Solar thermionic-thermoelectric generator for concentrating systems," *AIP Conf. Proc.*, vol. 1667, no. 1, p. 020007, Jun. 2015.

[23] A. Datas and C. Algora, "Development and experimental evaluation of a complete solar thermophotovoltaic system," *Prog. Photovolt. Res. Appl.*, vol. 21, no. 5, pp. 1025–1039, Aug. 2013.

[24] P. Calvani *et al.*, "Black diamond for solar energy conversion," *Carbon*, vol. 105, pp. 401–407, Aug. 2016.

[25] A. Bellucci, P. Calvani, M. Girolami, and D. M. Trucchi, "Defect engineering of diamond cathodes for high temperature solar cells," in *2015 IEEE 15th International Conference on Environment and Electrical Engineering (EEEIC)*, 2015, pp. 1616–1619.